TOWARDS IMPROVED SOLAR PV MODULE CHARACTERISATION: CORRELATING ELECTROLUMINESCENCE IMAGE DEFECTS WITH I-V CURVE CHARACTERISTICS USING A SEMANTIC SEGMENTATION-BASED MULTI-DEFECT DETECTION ALGORITHM

Frank Zandamela[1], Lawrence Pratt[1], May Siyasanga[1], Wisani Mkasi[1], and Thabang Mabeo[1]

[1] CSIR, Smart Places, Energy Research Centre, Pretoria 0001, South Africa; E-Mail: fzandamela@csir.co.za

[1] E-mail: lpratt@csir.co.za, smay@csir.co.za , hmkasi@csir.co.za, rmabeo@csir.co.za

Abstract: There has been significant research on the relationship between current-voltage (I-V) curve characteristics and electroluminescence (EL) module defects. Current methods use EL image pixels to develop features, which are then correlated with module I-V curve characteristics. In most cases, image thresholding is used to gather pixel information. These approaches have two major limitations. First, they lack generalisability, as imaging conditions may vary from module to module, and thresholding algorithms are often developed for specific types of defects or imaging conditions. Second, the correlation between specific types of defects and I-V features cannot be studied because all defects are grouped into one high-level defect detected by a sharp change in pixel intensity. In this paper, we conduct a correlation study between EL defects and I-V curve characteristics of photovoltaic (PV) modules that were exposed to accelerated stress testing. We correlate power loss and two common EL defects. The defects are detected and quantified using a prediction model based on semantic segmentation in which each pixel is assigned to one of multiple classes. Results obtained indicate that the defect detection tool can be used to correlate power loss with dark cells and cell cracks. A significant amount of variability in output power delta can be explained by defects detected by the prediction model (r^2 = 72%).

Keywords: Cell cracks; Electroluminescence image defect detection; I-V curve characteristics*; deep learning; PV module; semantic segmentation.*

1. Introduction

The ongoing adoption and installation of solar PV with the intention of moving to sustainable energy generation has necessitated the need to understand module lifetime performance and gain insights into the mechanisms causing module degradation [1]. Current-voltage (I-V) curve tracing and electroluminescence (EL) imaging are two of the commonly used techniques for characterising a PV module. I-V curve tracing performs a complete electrical sweep from short circuit current to open circuit voltage of an illuminated PV module [2]. The I-V curve characteristics alone cannot be used to determine specific degradation mechanisms leading to power loss. However, EL imaging rich spatial information that can help to understand the performance and condition of a module [3]. Due to the vital role that both I-V curve tracing and EL imaging play in the characterisation of a PV module, there has been a huge research effort aimed at finding the correlation between I-V curve characteristics of a PV module and the module defects found on the corresponding EL image [1]–[6]. Such studies can aid the development of algorithms that can estimate the I-V characteristics of a module. The ability to estimate module I-V features from EL images can enable high-speed in-situ power estimation for fielded PV modules and a framework for understanding large-scale mechanistic degradation of PV modules at high resolution. In addition, such a framework can be used across different facets of the PV community to improve speed, quality, and usefulness of cell and module-level image-based characterisation.

A host of the existing approaches use the EL image pixel intensities to derive hand-crafted features that describe the defects found on the EL image of the module. Approaches that use hand-crafted features derived from image pixel information have two major limitations. First, the approaches have limited or lack of generalising ability because imaging conditions may change from module to module and the thresholding algorithms are often developed for specific type of defects or imaging conditions. Second, the correlation between specific type of defects and the I-V features cannot be studied because all defects are grouped into one high-level defect that is detected by sharp

change in pixel intensity. Studying the correlation between specific defects and I-V features can help us understand low-level details about the performance of a module.

In this paper, we conduct a correlation study between two specific EL defects and I-V curve characteristics of PV modules that were exposed to accelerated stress testing at the CSIR PV Module Quality and Reliability Lab (PVQRL). The I-V data was measured on the indoor sun simulator and the EL defects were detected using a deep learning semantic segmentation-based model that was trained to detect and quantify common defects in solar cells.

2. Related work

The correlation of I-V curve characteristics and EL defects has received a lot of attention in the literature. The first work that investigated the impact of EL defects on module performance was presented by Köntges *et al.* [7]. In the paper, the direct impact of micro-cracks on the module power and the consequences after artificial aging were analysed. According to the results of the experiment, artificially initiated micro-cracks in the silicon wafer did not impair the electrical contact between cell fragments and did not reduce solar power generation by more than 2.5 %. It was found that cracked cells are correlated with power degradation after the accelerated ageing test, and that power loss follows a linear pattern over time. Since then, there has been significant research effort directed at investing the correlation of EL defects with I-V curve characteristics.

Existing methods investigate correlation between I-V curve characteristics and EL defects that are quantified using the pixel intensities of EL images. The I-V curve characteristics are typically obtained using a sun simulator. Typical characteristic values measured and derived from the module I-V curve include maximum power (Pmp), fill factor (FF), current at maximum power (Imp), voltage at maximum power (Vmp), current at short circuit (Isc), voltage at open circuit (Voc), series resistance (Rs), and shunt resistance (Rsh) [2]. To quantify EL defects, some researchers convert the EL images to grayscale and use the raw pixel intensities to calculate the median, mean, and standard deviation [2], [8]. For example, Karimi *et al.* [8] demonstrated the quantification of generalized and performance mechanism-specific EL image features using pixel intensity-based and machine learning classification algorithms. The research employed two stress testing methods: 3000 hours of damp heat exposure with measurements at 500-hour intervals for 15 modules, and 600 cycles of thermal cycling with measurements taken every 200 cycles for another 15 modules. This yielded 11,700 EL images from the 30 modules tested. Each cell-level image was analysed, resulting in four hand-crafted features being extracted, including the busbar corrosion ratio (BBCR). The research reported strong correlations between the features extracted from EL images and I-V characteristics. The study also uses a convolutional neural network to classify cells by the severity of busbar corrosion. In addition, researchers developed models to predict PV module I-V features from EL image characteristics, especially ribbon corrosion.

Some researchers [4], [9] also use image thresholding and edge detection techniques to enhance and localise module cracks. The area of a crack is then used to quantify the crack defect. For example, Wu *et al.* [4] used MATLAB's "im2bw(I, level)" function to perform image thresholding using different "level" values to capture and quantify module dark areas (cracks and inactive areas) using pixel intensity percentages. In their results, total pixel weight percentage of EL image dark areas and fill factor demonstrated a linear correlation with an r^2 value of 86.5 %. Likewise, Whitaker *et al.* [9] conducted a correlation study between I-V curve characteristics and EL image defects. The EL defects were quantified using an image thresholding algorithm called black top-hat transform. The black top-hat filter enhances dark cracks in a bright background; thus, it isolates darker pixels from brighter neighbouring pixels.

In this paper, we use a deep learning semantic segmentation EL defect detection tool to detect and quantify defects on EL images taken before and after accelerated stress testing. A study is then conducted to investigate possible correlations between the quantified defects and I-V curve characteristics of the PV modules. To the best of our knowledge, there is no study that investigates the correlation between EL defects quantified by a deep learning semantic segmentation algorithm.

3. Methodology

3.1. Solar cell defect detection overview

Solar cell defect detection (SCDD) on EL images is performed using a deep learning semantic segmentation model called Deeplabv3 [10]. The model was adapted for the task of defect detection on EL images using the source code provided by the authors on their official GitHub repository. The model was adapted using the three-step development process shown in Fig. 1. The reader is encouraged to refer to our previous work [11], [12] for details on the implementation and training details as they are beyond the scope of the current work.

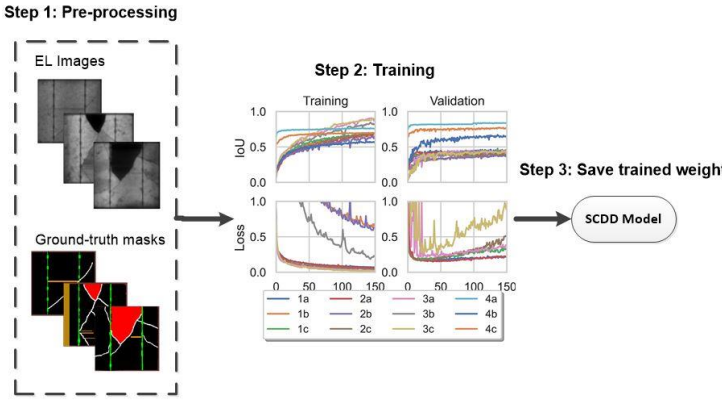

Fig. 1. Three-step development process of the SCDD model.

3.2. EL defects vs I-V curves correlation

The EL images and I-V curves were collected during a PV module reliability program conducted in 2019-2020 at the CSIR [13]. PV modules with four different 'bill-of-materials' (BOMs) were subjected to a series of accelerated stress tests according to the methods described in the IEC 61215:2016 international standard for PV module design qualification and type approval. The accelerated stress tests are designed to simulate real-world stresses in a controlled lab environment for certification testing. The PV Module Testing Protocol for Quality Assurance Programs described in the ANSI C450-18 is a public standard designed for long-term reliability testing of PV modules based on the IEC 61215 series in which the certification tests are conducted repeatedly. For example, a certification test per IEC 61215 requires 200 thermal cycles and the C450 requires 600 thermal cycles with a characterization sequence every 200 cycles. The characterisation sequence includes EL images and I-V measurements. The characterization sequence was conducted on each module as received at the lab and again after each step in the stress testing sequence, generating nearly 200 EL images and IV curves (Fig. 2).

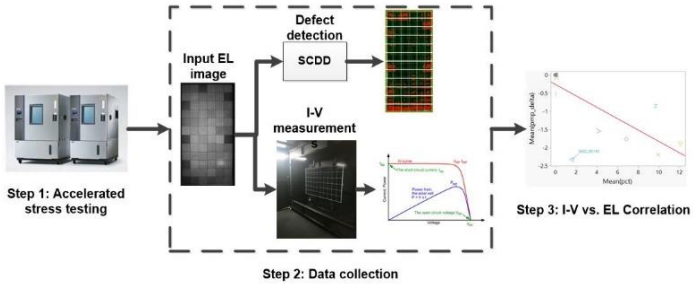

Fig. 2. Methodology used for the EL defects vs. I-V correlation study.

The I-V curves were generated on an indoor sun simulator at the CSIR PVQRL. The sun simulator is designed to measure the electrical characteristics over a range of temperatures and irradiance levels. A module is loaded into the integrated temperature chamber (Fig. 3) to control temperature while the irradiance level is controlled by the energy applied from a capacitor bank to the xenon arc lamp. The temperature chamber has a glass door to allow the light to hit the module and the irradiance level is monitored by a reference cell that is co-planar with the PV module. During a C450 reliability sequence, most I-V curves are conducted at standard test conditions (STC) defined as 1000 W/m^2, 25 °C cell temperature, and a light spectrum consistent with the natural sunlight at an airmass of 1.5.

Fig. 3. PV module mounted inside the sun simulator thermal chamber with glass door.

The correlation analysis was conducted using simple linear regression and summarized by the coefficient of determination, or the square of the Pearson's Correlation Coefficient (r^2). The dataset consisted of matched pairs for each module at each characterization step. The pairs consisted of an IV characteristic and an output from the SCDD model. Table 1 shows a subset of the data used in this study. Row 1 shows a record for the 'dark cell' defect on Module 1 at the initial inspection. The initial maximum power (Pmp) serves as the reference point for subsequent IV measurement, so the delta to initial = 0. The percentage defective shows the output of the SCDD model averaged over all the cells in the module. At this stage, the SCDD model did not detect any 'dark cell' defects in any of the cells. The second row shows the results on the same module after the potential inducted degradation (PID) stress test. The module power decreased by 6.8% and the SCDD model predicted 1.77% of the pixels were likely from dark cells, on average. The bottom half of the table shows a similar example for one module after the thermal cycling sequence. After 600 thermal cycles (TC600), the module power decreased by 1.1 % and the percentage defective increased to 0.52 %. This study focuses on maximum power measurements (Pmp) versus dark cells after PID and cracks after thermal cycling.

Table 1. Sample records of the dataset used for the correlation analysis.

Defect	Module ID	Sequence	Pmp Delta to Initial (%)	Percentage Defective (%)
Dark cell	1	Initial	0.0	0.00
Dark cell	1	Post PID	6.8	-1.77
Dark cell	2	Initial	0.0	0.00
Dark cell	2	Post PID	9.9	-2.19
Crack	1	Initial	0.0	0.06
Crack	1	Post TC200	-0.2	0.07
Crack	1	Post TC400	-0.5	0.48
Crack	1	Post TC600	-1.1	0.52

The r^2 value from the linear regression quantifies the proportion of the variation in the dependent variable (y-axis) explained by the independent variable (x-axis). For example, Fig. 4 shows the least squares line for maximum power (Pmp) versus current at maximum power (Imp) for a subset of the modules analysed in this research. The r^2= 0.99, meaning 99 % of the variability in the Pmp can be explained by the variability in Imp. While correlation does not prove causation, in the case of I-V characteristics this relationship does imply causation because a higher current output will lead to higher power output.

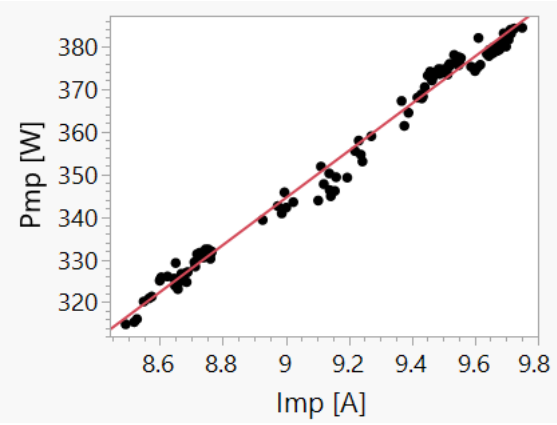

Fig. 4. Simple linear regression of maximum power (Pmp) delta to initial versus current at maximum power (Imp) delta to initial (r^2 = 0.99).

Table 2 shows the key statistics for the analysis of variance from the linear regression model. The sum of squares error (SSE) quantifies the residual errors, specifically the value represents the sum of the squared residuals. The sum of squares total (SST) quantifies the variance in the Pmp, specifically the value represents the sum of squared differences between the Pmp and the average of the Pmp. The sun of squares model (SSM) is the difference between the SST and the SSE. The ratio of the SSM over SST equals the r^2. In this case, 99 % of the variability in the Pmp is explained by the Imp.

Table 2 Analysis of variance summary statistics for the linear regression analysis.

Description	Value
Error Sum of Squares (SSE)	350 223
Model Sum of Squares (SSM)	31 562 191
Total Sum of Squares (SST)	31 912 413
R^2	0.99

4. Results and analysis

4.1. Module output power vs. dark cells post PID

Fig. 5 shows the correlation between module power loss (delta to initial Pmp) and the percentage of dark cell pixels predicted by the SCDD model. A subset of the dataset was described in Section 3.2 for clarity. An r^2 value of 55% was obtained from the analysis of variance table as described in Table 2. This indicates that 55% of the decrease in Pmp can be explained by the increase in the dark cell percentage. The point representing SASC_00145 module was an outlier with respect to the regression model. With the outlier excluded, an r^2 value of 78% percentage was obtained. This demonstrates the significant impact the outlier had on the correlation analysis. Further investigations were made to understand the behaviour of the SASEC_00145 observation.

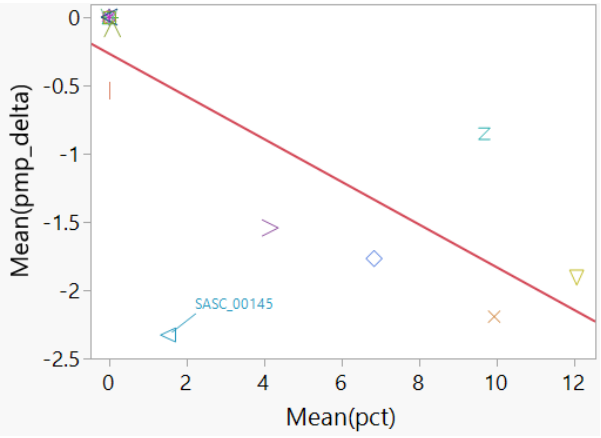

Fig. 5. Regression analysis between delta output power and percentage of dark cells predicted by SCDD.

We investigated the effect of pre-processing methods applied to the EL images before prediction by the SCDD tool to better understand the SASEC_00145 outlier. Specifically, we studied the influence of the brightness of an EL image on the ability of the SCDD tool to predict and quantify dark cells. Fig. 6 shows the correlation between the module power loss (delta to initial Pmp) and the percentage of dark cell pixels predicted by the SCDD model after reducing the brightness of the original EL image of the SASEC_00145 PV module by 50%. The percentage of dark cell pixels predicted by the SCDD model increased after reducing the brightness, and the resulting r^2 value increased by 17% (from 55% to 72%). This suggests that pre-processing methods that change the brightness of EL images impact the prediction of dark cells.

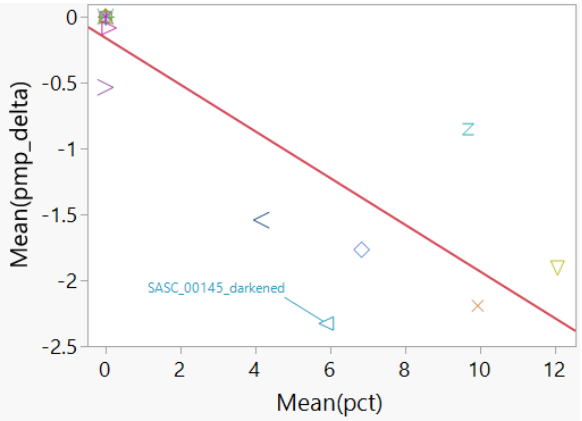

Fig. 6. Regression analysis between delta output power and percentage of dark cells predicted by SCDD after darkening the PV module.

The bias current applied during EL imaging can also impact pixel brightness. Fig. 7 shows the change in the percentage of dark cell pixels in the pre- and post-stress EL images recorded at 100 % of Isc current and in the post-stress EL image at 10 % of Isc current. The percentage of pixels predicted as dark cells increases significantly when the current bias is decreased from 100 % of Isc current to 10 % of Isc current, as per the international standard. The IEC TS 62804-1 describes the test methods for the detection of potential-induced degradation. In that technical specification, the test sequence includes EL imaging at both 100 % of Isc current and 10 % of Isc current because the PID degradation is more easily seen to the human observer at the low bias setting It follows that the SS model would also detect more dark cell pixels in images taken at low bias. Unfortunately, the pre-stress EL images at 10% of Isc were not available to assess the percentage of dark cell pixels at that bias current prior to the stress.

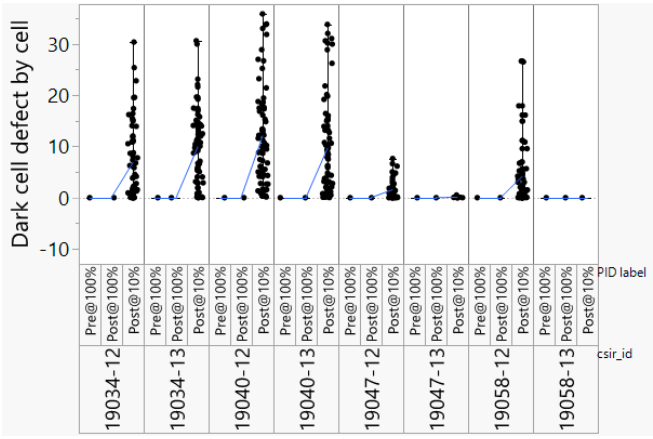

Fig. 7. Percentage of dark cells post PID at different levels of bias current.

4.2. Module output power vs. cracks after thermal cycling

Fig. 8 shows the correlation between module power loss (delta to initial Pmp) and the percentage of crack pixels predicted by the SCDD model for each module from one BOM that was subjected to thermal cycling. Based on the Pmp delta and cracked cell percentage values, an r^2 value of 55% was obtained. This indicates that 55% of the change in Pmp can be explained by the change in the percentage of crack pixels predicted by the SCDD model.

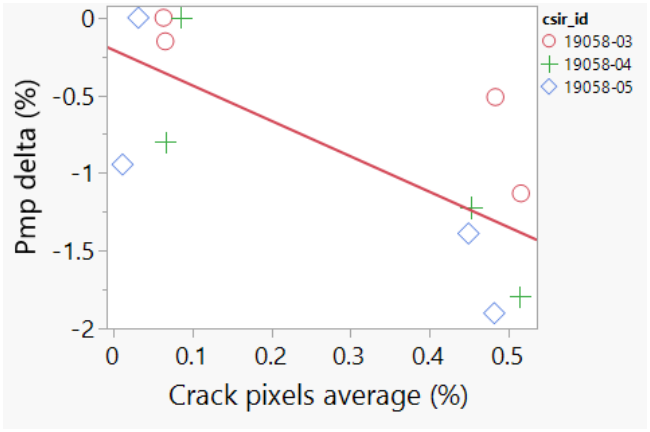

Fig. 8. Regression analysis between Pmp delta and crack pixels average post thermal cycling.

Fig. 9 shows the evolution of cell cracks on the three PV modules from one BOM during 600 hours of thermal cycling, using steps of 200 thermal cycles. From this figure, it can be observed that all three PV modules developed cracks after TC400. This was not expected since thermal cycling does not typically cause cracks, and none of the modules from the other three BOMs developed significant cracks. Interestingly, the cracks showed a similar pattern across all three modules with long, 45 ° diagonal cracks developing in the top left and bottom right corners.

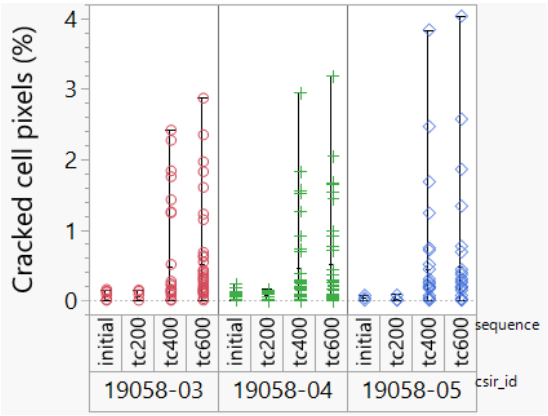

Fig. 9. Variation of the percentage of cracked cells at 0, 200, 400, and 600 thermal cycles.

The sensitivity of crack detection to brightness post thermal cycling was also investigated. It was found that crack detection is robust to any brightness changes applied to the original image during pre-processing.

5. Conclusion

This work investigated linear correlations between the output of a semantic segmentation model trained to detect defects in EL images and the corresponding IV characteristics of PV modules exposed to accelerated stress testing. The output power of PV modules that were subjected to damp heat and thermal cycling was correlated to the percentage of dark cells and the percentage of cracks, respectively. The results suggest that a significant amount of variability in output power loss can be explained by defects detected by the SCDD tool, although causation should not be implied. In addition, it was found that the prediction of dark cells using the SCDD tool is susceptible to brightness changes in the EL image made during post-processing and the electrical current bias applied during imaging. In contrast, crack detection is robust to brightness changes.

Future work will include further investigations on the sensitivity of predictions using the SCDD model to image preprocessing.

Acknowledgements

The authors wish to thank the CSIR and the Centre for High Performance Computing (CHPC) for measurement equipment, test samples, and computing resources. The authors also wish to thank David Torpey for technical support in the development of the SCDD model.

References

[1] R. Asadpour, D. B. Sulas-Kern, S. Johnston, J. Meydbray, and M. A. Alam, “Dark Lock-in Thermography Identifies Solder Bond Failure as the Root Cause of Series Resistance Increase in Fielded Solar Modules,” IEEE Journal of Photovoltaics, vol. 10, no. 5, pp. 1409–1416, Sep. 2020.

[2] J. S. Fada et al., "Correlation of I-V Curve Parameters with Module-Level Electroluminescent Image Data Over 3000 Hours Damp-Heat Exposure," 2017 IEEE 44th Photovoltaic Specialist Conference (PVSC), Washington, DC, USA, 2017, pp. 2697-2701.

[3] A. M. Karimi et al., "Generalized and Mechanistic PV Module Performance Prediction From Computer Vision and Machine Learning on Electroluminescence Images," in IEEE Journal of Photovoltaics, vol. 10, no. 3, pp. 878-887, May 2020.

[4] Wu, Jiawei, et al. "Durability evaluation of PV modules using image processing tools." New Concepts in Solar and Thermal Radiation Conversion and Reliability. Vol. 10759. SPIE, 2018. vol. 1075915, no. September 2018, p. 36, 2018.

[5] M. Hoffmann et al., “Deep-learning-based pipeline for module power prediction from electroluminescense measurements,” Progress in Photovoltaics, vol. 29, no. 8, pp. 920–935, May 2021.

[6] V. Kumar and P. Maheshwari, “Advanced analytics on IV curves and electroluminescence images of photovoltaic modules using machine learning algorithms,” Progress in Photovoltaics: Research and Applications, Sep. 2021.

[7] M. Köntges, I. Kunze, S. Kajari-Schröder, X. Breitenmoser, and B. Bjørneklett, “The risk of power loss in crystalline silicon based photovoltaic modules due to micro-cracks,” Solar Energy Materials and Solar Cells, vol. 95, no. 4, pp. 1131–1137, Apr. 2011.

[8] A. M. Karimi *et al.*, “Generalized and Mechanistic PV Module Performance Prediction from Computer Vision and Machine Learning on Electroluminescence Images,” *IEEE J. Photovoltaics*, vol. 10, no. 3, pp. 878–887, 2020.

[9] C. M. Whitaker, B. G. Pierce, A. M. Karimi, R. H. French, and J. L. Braid, “PV Cell Cracks and Impacts on Electrical Performance,” *Conf. Rec. IEEE Photovolt. Spec. Conf.*, vol. 2020-June, pp. 1417–1422, 2020.

[10] L. C. Chen, Y. Zhu, G. Papandreou, F. Schroff, and H. Adam, “Encoder-decoder with atrous separable convolution for semantic image segmentation,” *Lect. Notes Comput. Sci. (including Subser. Lect. Notes Artif. Intell. Lect. Notes Bioinformatics)*, vol. 11211 LNCS, pp. 833–851, 2018.

[11] L. Pratt, J. Mattheus, and R. Klein, “A benchmark dataset for defect detection and classification in electroluminescence images of PV modules using semantic segmentation,” *Systems and Soft Computing*, vol. 5. 2023.

[12] L. Pratt, D. Govender, and R. Klein, “Defect detection

and quantification in electroluminescence images of solar PV modules using U-net semantic segmentation," *Renewable Energy*, vol. 178. pp. 1211–1222, 2021.

[13] L. Pratt, M. B. Ayanna, S. I. May, W. Mkasi, L. Maweza, and K. Roro, "PV MODULE RELIABILITY SCORECARD - ROUND 1," pp. 1–7.